

Species Abundance Distribution and Species Accumulation Curve: A General Framework and Results

Cheuk Ting LI

Department of Information Engineering,
The Chinese University of Hong Kong.

ctli@ie.cuhk.edu.hk

Kim-Hung LI

Asian Cities Research Centre Ltd., Hong Kong.

khli@acrc.hk

November 1, 2021

Abstract

We build a general framework which establishes a one-to-one correspondence between species abundance distribution (SAD) and species accumulation curve (SAC). The appearance rates of the species and the appearance times of individuals in each species are modeled as Poisson processes. The number of species can be finite or infinite. We introduce a linear derivative ratio family of models, LDR_1 , of which the ratio of the first and the second derivatives of the expected SAC is a linear function. A $D1/D2$ plot is proposed to detect this linear pattern in the data. The SAD of LDR_1 is the Engen's extended negative binomial distribution, and the SAC encompasses several popular parametric forms including the power law. Family LDR_1 is extended in two ways: LDR_2 which allows species with zero detection probability, and RDR_1 where the derivative ratio is a rational function. We also consider the scenario where we record only a few leading

appearance times of each species. We show how maximum likelihood inference can be performed when only the empirical SAC is observed, and elucidate its advantages over the traditional curve-fitting method.

Keywords: Engen’s extended negative binomial distribution; Power law; Rarefaction curve; Species richness; Species-time relationship.

1 Introduction

Estimating the number of distinct classes in a population is a problem encountered in many fields. We may be interested in the number of words a person know from his/her writings [Efron and Thisted, 1976], the number of illegal immigrants from the apprehension records [Böhning and Schön, 2005], the number of distinct attributes in a database [Haas et al., 1995, Deolalikar and Laffitte, 2016], or the number of distinct responses to a crowdsourcing query [Trushkowsky et al., 2012]. Among different applications, species richness is the one that receives most attention. For this reason, it is chosen as the theme of this paper with the understanding that the proposed framework and methods are applicable in other applications as well. The problem is challenging because we cannot exclude with confidence the possibility that there are huge number of extremely rare classes.

Understanding the species abundance in an ecological community has long been an important task for ecologists. Such knowledge is paramount in conservation planning and biodiversity management [Matthews and Whittaker, 2015]. An exhaustive species inventory is too labor and resource intensive to be practical. Information about species abundance can thus be acquired mainly through a survey.

Let $N = (N_0, N_1, \dots)$ where N_k is the number of species in a community that are represented exactly k times in a survey. We do not observe the whole N , but $\tilde{N} = (N_1, N_2, \dots)$ which is the zero-truncated N . In other words, we do not know how many species are not seen in the survey. We call the vector \tilde{N} , the frequency of frequencies (FoF) [Good, 1953].

A plethora of species abundance models have been proposed for \tilde{N} . Comprehensive review of the field can be found in McGill et al. [2007] and Matthews and Whittaker

[2014]. A typical assumption in purely statistical models is that

$$\tilde{N} \mid N_+ \sim \text{Multinomial}(N_+, p), \quad (1)$$

where $N_+ = \sum_{k=1}^{\infty} N_k$ is the total number of recorded species, and $p = (p_1, p_2, \dots)$ is a probability vector, such that p_k is the probability for a randomly selected recorded species to be observed k times in the study for $k = 1, 2, \dots$. We call this vector p , the species abundance distribution (SAD). Species accumulation curve (SAC) is another tool in the analysis of species abundance data. The survey is viewed as a data-collection process in which more and more sampling effort is devoted. SAC is the number of recorded species expressed as a function of the amount of sampling effort.

Despite the different emphases of the SAD and the SAC, the two approaches have an overlapped target: Estimating D , the total number of species in the community. For SAD, it means estimating N_0 , the number of unseen species as $D = N_0 + N_+$. In SAC, D is interpreted as the total number of seen species when the sampling effort is unlimited. Both involve risky extrapolation.

As SAD depends largely on the sampling effort, it is necessary to include sampling effort explicitly in the model in order to make comparison of different SADs possible. This addition establishes a link between SAD and SAC. Sampling effort can be of continuous type, such as the area of land or the volume of water inspected, or the duration of the survey. Discrete type sampling effort can be the sample size. To emphasize the sampling effort considered, the SAC is called species-time curve, species-area curve, or species-sample-size curve when the sampling effort is time, area sampled, or sample size respectively. Species-area curve has been studied extensively in the literature. Review of it can be found in Tjørve [2003, 2009], Dengler [2009] and Williams et al. [2009]. In this paper, we use time as the measure of sampling effort. We consider the vector N to be a function of the time t , denoted as $N(t)$. Notations N_k , \tilde{N} , N_+ , p and p_k are likewise denoted as $N_k(t)$, $\tilde{N}(t)$, $N_+(t)$, $p(t)$ and $p_k(t)$ respectively. An SAC is $N_+(t)$ as a function of t . Because of the great similarity of the species-time relationship and species-area relationship [Preston, 1960, Magurran, 2007], time and area are treated as if they are interchangeable in this paper. When SAC is species-area curve, we refer to the Type I species-area curve [Scheiner, 2003], where the areas sampled are nested (smaller areas are included in larger areas), resulting in a curve

that is always nondecreasing. Throughout the paper, we denote the time at which the survey starts as time 0, and the time at which the data are summarized and analyzed as time $t_0 > 0$.

It is easy to discover that $N_0(t_0)$, which is a quantity of interest plays no role in model (1). A common and stronger assumption is that $N(t_0)$ follows a multinomial distribution. A reason why (1) is used instead of this stronger version is that the latter assumes finite D . Finite D is commonplace in SAD approach although no consensus has been reached. Empirically, log-series distribution, a SAD that assumes infinite D , is one of the most successful models. Many SACs do not have asymptote. It is common that the number of rare species is large, and shows no sign to decrease. In Bayesian nonparametric approach in genomic diversity study, Poisson-Dirichlet process which assumes infinite D is used (see for example Lijoi, Mena, and Prünster [2007], Favaro et al. [2009]). In reality, the existence of transient species (species which are observed erratically and infrequently [Novotny and Basset, 2000]), and the error in the species identification process (a well-known example is the missequencing in pyrosequencing of DNA [Dickie, 2010, Quince et al., 2011]) are continual sources of rare species making the species number larger than expected. Taking into consideration that the method may be applied in fields other than species richness estimation, we decide not to exclude the possibility of infinite D from the framework.

An extreme kind of rare species is species with zero detection probability. We call such species, zero-probability species, and all other species, positive-rate species. Zero-probability species can either be seen only once or unseen in the survey. If there are finite number of zero-probability species, the probability of observing any of them is zero. Therefore, if a zero-probability species is observed in a study, it is almost sure that there are infinite number of them.

In this paper, we propose a new model for the sampling process, called the mixed Poisson partition process in Section 2. It can handle the case where D is finite or infinite, and allows existence of zero-probability species. We study $\tilde{N}(t)$ in Section 3. In Section 4, we consider the expected species accumulation curve (ESAC). It is shown that there is one-to-one correspondence between a mixed Poisson partition process and an ESAC which is a Bernstein function that passes through the origin. In Section 5,

we introduce LDR_1 , a family of ESAC. The SAD of LDR_1 is the Engen's extended negative binomial distribution. This family has an attractive property that the ratio of the first and the second derivatives of the ESAC is a linear function of t . A D1/D2 plot is proposed to detect this linear relation. We extend LDR_1 to LDR_2 which allows zero-probability species. In Section 6, LDR_1 is generalized so that the derivative ratio is a rational polynomial instead of a linear function of t . Four real data are analyzed in Section 7 to demonstrate the applications of the proposed models. Section 8 is on sampling designs. In Section 9, we consider the maximum likelihood approach on the empirical SAC. We give a conclusion in Section 10.

2 Mixed Poisson Partition Process

In a species richness survey, individuals are recorded as a labeled point process, where each point has two attributes: its time of observation, and which one of the (finitely or infinitely many) species it belongs. A partitioned point process is a random element $G = \{\eta_1, \eta_2, \dots, \eta_D\}$, where each η_i is the set of times at which individuals of species i are observed and D is a random nonnegative integer which can be infinite. Sample G is an unordered set, and the labels i of η_i has no meaning. For example, if D is a fixed positive integer, and the individuals of each species, say species i , are observed independently according to a Poisson process with rate λ_i , then η_i is generated according to a Poisson process with rate λ_i , and $G = \{\eta_1, \dots, \eta_D\}$. It reduces to the mixed Poisson model when we further assume that $\lambda_1, \dots, \lambda_D$ are random sample from a mixing distribution. In this paper, we will consider the following process in which D is random.

Definition: (Mixed Poisson partition process) A mixed Poisson partition process, G , is characterized by a species intensity measure ν , which is a measure over $\mathbb{R}_{\geq 0}$, the set of all nonnegative real numbers, satisfying

$$\int_0^\infty \min\{1, \lambda^{-1}\} \nu(d\lambda) < \infty. \quad (2)$$

The definition of a mixed Poisson partition process consists of three steps:

1. (Generation of positive rates of species) Given ν , define $\tilde{\nu}$ to be a measure over

$\mathbb{R}_{>0}$ ($\mathbb{R}_{>0}$ is the set of positive real numbers) by $\tilde{\nu}(d\lambda) = \nu(d\lambda)/\lambda$, (i.e., $d\tilde{\nu}/d\nu = 1/\lambda$ for $\lambda > 0$). Generate $\lambda_1, \lambda_2, \dots$ (a finite or countably infinite sequence) according to a Poisson process with intensity measure $\tilde{\nu}$.

2. (Generation of individuals of positive-rate species) For each λ_i in Step 1, we generate η_i (independently across i) according to a Poisson process with rate λ_i .
3. (Generation of individuals of zero-probability species) We generate η_0 according to a Poisson process with rate $\nu(\{0\})$, independent of η_1, η_2, \dots . This represents the times of appearance for all the zero-probability species.

Finally, we take $G = \{\eta_1, \eta_2, \dots\} \cup \eta_0$. For any $i \geq 1$, all points in η_i are from the same species, whereas each point in η_0 is from a different species (we use a slight abuse of notation to treat each point in η_0 as a point process with only one point).

Similar to Step 1, Zhou, Favaro, and Walker [2017] also considered the species to be generated according to a random process. However, their model does not involve time (or area), and hence does not describe the species-time relationship (or species-area relationship). Although their model includes cases where D is infinite, it fails to handle zero-probability species.

We observe a mixed Poisson partition process in time interval $[0, t_0]$. In this paper, measure ν is assumed having a known parametric form, and our task is to estimate the parameters that govern ν . Measures ν and $\tilde{\nu}$ may be finite or infinite. As the expected number of individuals seen in time interval $[0, t]$ is equal to $t\nu(\mathbb{R}_{\geq 0})$ (see (6) in Section 3), the finiteness of ν means that this expected value is finite for any finite t . If $\tilde{\nu}$ is finite, the expected number of positive-rate species in the community is finite. From Step 3 in the definition, if $\nu(\{0\}) > 0$, there are infinite number of zero-probability species and they arrive at a constant rate. With probability one, D is finite if and only if $\nu(\{0\}) = 0$ and $\tilde{\nu}(\mathbb{R}_{>0}) = \int_0^\infty (1/\lambda)\nu(d\lambda) < \infty$ (see (7) in Section 3). In such case, D follows a $\text{Poisson}(\int_0^\infty (1/\lambda)\nu(d\lambda))$ distribution. Measure $\tilde{\nu}$ specifies the distribution of the rates of positive-rate species. More precisely, $\tilde{\nu}([\lambda_0, \lambda_1])$ with $\lambda_0 > 0$ is the average number of species with rate in $[\lambda_0, \lambda_1]$. Measure ν specifies the distribution of the rates of the species of the individuals including those of the zero-probability species. More precisely, $\nu([\lambda_0, \lambda_1])$ is the average number of individuals (per unit time) belonging to

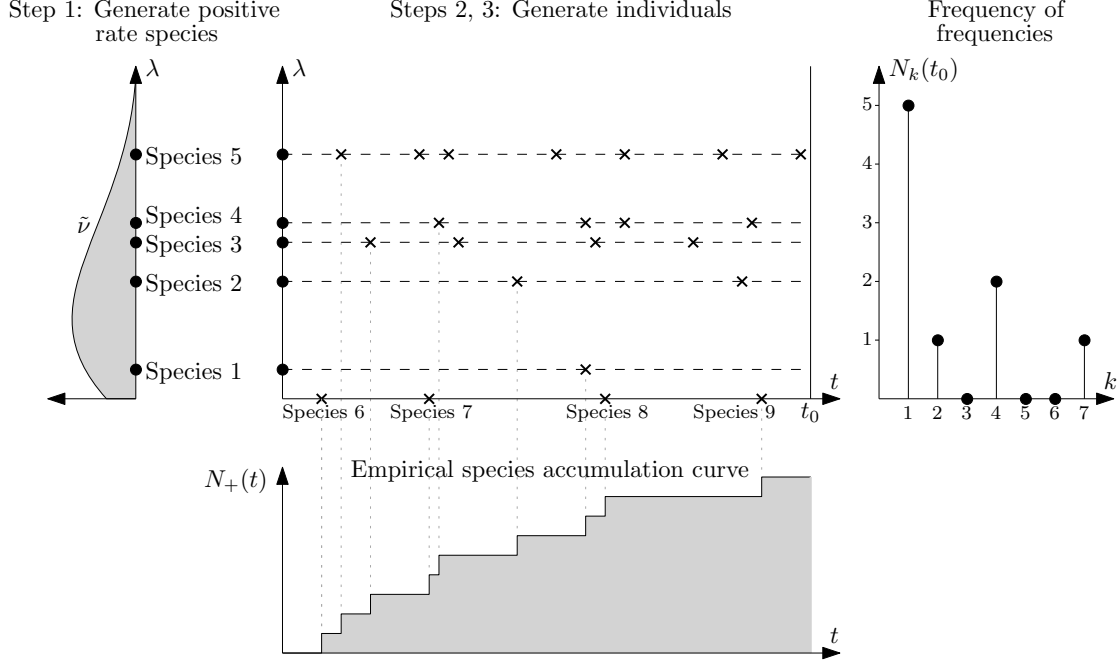


Figure 1: An illustration of the mixed Poisson partition process. In step 1, we generate the rates λ_i of the positive-rate species according to a Poisson process with intensity measure $\tilde{\nu}$. If $\tilde{\nu}(\mathbb{R}_{>0}) < \infty$, then this is equivalent to first generating n_{pos} , the number of positive-rate species according to $\text{Poisson}(\tilde{\nu}(\mathbb{R}_{>0}))$, and then generating a random sample $\lambda_1, \dots, \lambda_{n_{pos}}$ of size n_{pos} from the probability measure $\tilde{\nu}/\tilde{\nu}(\mathbb{R}_{>0})$. In step 2, we generate the individuals of species i according to a Poisson process with rate λ_i for $i = 1, \dots, n_{pos}$. In step 3, we generate the individuals of zero-probability species (species 6 to 9 in the figure) according to a Poisson process with rate $\nu(\{0\})$.

species whose rates lie in $[\lambda_0, \lambda_1]$. Condition (2) is essential because it is equivalent to the finiteness of the ESAC (i.e. $E(N_+(t)) < \infty$ for any finite nonnegative t) as will be proved in Section 3. Figure 1 illustrates the generation of the mixed Poisson partition process. An alternative equivalent definition that unifies the three steps in the definition into one is given in Appendix A.

3 Frequency of Frequencies

The FoF, $\tilde{N}(t_0)$ is a sufficient statistic for a realization of a mixed Poisson partition process in time interval $[0, t_0]$. Understanding the probabilistic properties of $\tilde{N}(t)$ is

essential. Let $\lambda_1, \lambda_2, \dots$ be the values drawn from a Poisson process with intensity measure $\tilde{\nu}$. For each λ , it contributes to one of the counts $N_k(t)$, where k follows a Poisson distribution $\text{Poisson}(\lambda t)$. By the splitting property of Poisson process, their total contribution to $N_k(t)$ follows $\text{Poisson}\left(\int (\lambda t)^k (k!)^{-1} \exp(-\lambda t) \tilde{\nu}(d\lambda)\right)$ distribution independent across k . We call species with observed frequency one, singleton, and $N_1(t)$, the singleton count. For the contribution of $\nu(\{0\})$ to $N_k(t)$, η_0 is a Poisson process with rate $\nu(\{0\})$. It affects only the singleton count by increasing its value by a random variable with distribution $\text{Poisson}(\nu(\{0\})t)$. Therefore,

$$\begin{aligned} N_k(t) &\sim \text{Poisson}\left(\int \frac{(\lambda t)^k \exp(-\lambda t)}{k!} \tilde{\nu}(d\lambda) + \mathbf{1}\{k=1\} \nu(\{0\})t\right) \\ &= \text{Poisson}\left(\int \frac{\lambda^{k-1} t^k \exp(-\lambda t)}{k!} \nu(d\lambda)\right), \end{aligned} \quad (3)$$

where $\mathbf{1}\{.\}$ is the indicator function. We use the convention $0^0 = 1$. As $N_+(t) = \sum_{k=1}^{\infty} N_k(t)$ and all $\{N_k(t)\}$ are independent,

$$N_+(t) \sim \text{Poisson}\left(\sum_{k=1}^{\infty} \int \frac{\lambda^{k-1} t^k \exp(-\lambda t)}{k!} \nu(d\lambda)\right) = \text{Poisson}\left(\int \frac{1 - \exp(-\lambda t)}{\lambda} \nu(d\lambda)\right), \quad (4)$$

where we assume $(1 - \exp(-\lambda t))/\lambda = t$ when $\lambda = 0$. From (3) and (4),

$$E(N_k(t)) = \int \frac{\lambda^{k-1} t^k \exp(-\lambda t)}{k!} \nu(d\lambda), \text{ for } k \geq 1, \text{ and } E(N_+(t)) = \int \frac{1 - \exp(-\lambda t)}{\lambda} \nu(d\lambda). \quad (5)$$

Condition (2) is equivalent to $E(N_+(t)) < \infty$ for $t \geq 0$ because under Condition (2),

$$\int \frac{1 - \exp(-\lambda t)}{\lambda} \nu(d\lambda) \leq \int \min\{t, \lambda^{-1}\} \nu(d\lambda) \leq \max\{t, 1\} \int \min\{1, \lambda^{-1}\} \nu(d\lambda) < \infty$$

for $t \geq 0$, and if $E(N_+(1)) < \infty$, then

$$\int \min\{1, \lambda^{-1}\} \nu(d\lambda) \leq \frac{1}{1 - \exp(-1)} \int \frac{1 - \exp(-\lambda)}{\lambda} \nu(d\lambda) = \frac{E(N_+(1))}{1 - \exp(-1)} < \infty.$$

Let $S(t) = \sum_{k=1}^{\infty} k N_k(t)$ be the number of individuals observed before time t . Then

$$E(S(t)) = \sum_{k=1}^{\infty} k \int \frac{\lambda^{k-1} t^k \exp(-\lambda t)}{k!} \nu(d\lambda) = t \int \nu(d\lambda). \quad (6)$$

Furthermore,

$$E(D) = \lim_{t \rightarrow \infty} E(N_+(t)) = \lim_{t \rightarrow \infty} \int \frac{1 - \exp(-\lambda t)}{\lambda} \nu(d\lambda) = \begin{cases} \infty & (\nu(\{0\}) > 0) \\ \int \tilde{\nu}(d\lambda) & (\nu(\{0\}) = 0). \end{cases} \quad (7)$$

It is easy to see that model (1) is valid under the framework, and

$$p_k(t) = \frac{E(N_k(t))}{E(N_+(t))} = \frac{\int (k!)^{-1} \lambda^{k-1} t^k \exp(-\lambda t) \nu(d\lambda)}{\int \lambda^{-1} (1 - \exp(-\lambda t)) \nu(d\lambda)} \quad (k = 1, 2, \dots). \quad (8)$$

If $E(D)$ is finite, $\lim_{t \rightarrow \infty} p_k(t) = 0$ for any fixed k .

Let $n_k(t_0)$ be the observed $N_k(t_0)$ for $k = 1, 2, \dots$ and $\tilde{n}(t_0) = \{n_k(t_0)\}_{k \geq 1}$. From (3), the joint probability mass function of $\tilde{N}(t_0)$ is

$$P(\tilde{N}(t_0) = \tilde{n}(t_0) \mid \nu) = \exp(-E(N_+(t_0))) \prod_{k=1}^{\infty} \frac{(E(N_k(t_0)))^{n_k(t_0)}}{n_k(t_0)!}.$$

In terms of the expected FoF, the log-likelihood function is

$$\log(\mathcal{L}(\nu \mid \tilde{n}(t_0))) = -E(N_+(t_0)) + \sum_{k=1}^{\infty} n_k(t_0) \log(E(N_k(t_0))). \quad (9)$$

In terms of $p(t_0)$ and $E(N_+(t_0))$, it is

$$\log(\mathcal{L}(p(t_0), E(N_+(t_0)) \mid \tilde{n}(t_0))) = -E(N_+(t_0)) + n_+(t_0) \log(E(N_+(t_0))) + \sum_{k=1}^{\infty} n_k(t_0) \log(p_k(t_0)).$$

If the unknown vector $p(t_0)$ and the quantity $E(N_+(t_0))$ are unrelated, the above expression of the log-likelihood function implies that the maximum likelihood estimator (MLE) of $p(t_0)$ is the conditional maximum likelihood estimator (conditional on the observed $n_+(t_0)$) of the multinomial distribution in (1). The MLE of $E(N_+(t_0))$ is $n_+(t_0)$, i.e. the MLE of the expected number of seen species before time t_0 is equal to the observed number of seen species before time t_0 .

4 Expected Species Accumulation Curve

The empirical SAC is $N_+(t)$. We call its expectation, expected SAC (ESAC), and denote it as $\psi(t)$. Condition (2) guarantees that $\psi(t)$ is finite for any finite t . From Equation (5),

$$\psi(t) = \int \frac{1 - \exp(-\lambda t)}{\lambda} \nu(d\lambda) = \nu(\{0\})t + \int (1 - \exp(-\lambda t)) \tilde{\nu}(d\lambda). \quad (10)$$

Hence, for $k = 1, 2, \dots$,

$$\psi^{(k)}(t) = \int (-\lambda)^{k-1} \exp(-\lambda t) \nu(d\lambda), \quad (11)$$

where $g^{(m)}(t)$ stands for the m -order derivative of function $g(t)$. From (11), $\psi(t)$ is a Bernstein function [Schilling, Song, and Vondracek, 2012] (a function $g(t)$ is a Bernstein function if it is a nonnegative real-valued function on $[0, \infty)$ such that $(-1)^k g^{(k)}(t) \leq 0$ for all $k \geq 1$). In considering a restricted model, Boneh, Boneh, and Caron [1998] found that $(-1)^{k+1} \psi^{(k)}(t) \geq 0$ and called it, alternating copositivity. Every Bernstein function $g(t)$ with $g(0) = 0$ has a unique Lévy-Khintchine representation

$$g(t) = \tau t + \int_0^\infty (1 - \exp(-\lambda t)) \mu(d\lambda), \quad (12)$$

where $\tau \geq 0$, and μ is a measure over $[0, \infty)$ such that $\int_0^\infty \min\{1, \lambda\} \mu(d\lambda) < \infty$. Comparing (10) and (12), we have $\tau = \nu(\{0\})$ and $\mu = \tilde{\nu}$. The condition $\int_0^\infty \min\{1, \lambda\} \mu(d\lambda) < \infty$ is equivalent to Condition (2).

From (5) and (11), for $k = 1, 2, \dots$

$$\psi^{(k)}(t) = (-1)^{k+1} \frac{k!}{t^k} E(N_k(t)). \quad (13)$$

Analogous expression for (13) appears in Béguinot [2016] as an approximate formula under the multinomial model for fixed total number of observed individuals for the species-sample-size curve with the derivative operator replaced by the difference operator. From (9), the log-likelihood function can be re-expressed as

$$\log(\mathcal{L}(\psi \mid \tilde{n}(t_0))) = -\psi(t_0) + \sum_{k=1}^{\infty} n_k(t_0) \log(|\psi^{(k)}(t_0)|). \quad (14)$$

Let us consider the power expansion of $\psi(t)$.

$$\begin{aligned} \psi(t) &= \int \frac{1 - \exp(-\lambda t)}{\lambda} \nu(d\lambda) - \int \frac{(\exp(\lambda(t_0 - t)) - 1) \exp(-\lambda t_0)}{\lambda} \nu(d\lambda) \\ &= E(N_+(t_0)) + \sum_{k=1}^{\infty} (-1)^{k+1} E(N_k(t_0)) \left(\frac{t}{t_0} - 1 \right)^k. \end{aligned} \quad (15)$$

Equation (15) can be re-expressed as

$$\psi(t) = E(N_+(t_0)) \left(1 - \sum_{k=1}^{\infty} p_k(t_0) \left(1 - \frac{t}{t_0} \right)^k \right). \quad (16)$$

Equations (8), (12), and (16) establishes the one-to-one correspondence among the following three parametrizations of the mixed Poisson partition process: (i) the species intensity measure ν (or $\nu(0)$ and $\tilde{\nu}$ as a whole), (ii) the ESAC $\psi(t)$ which is a Bernstein

function passing through the origin, and (iii) the SAD $p(t_0)$ in the form of (8) together with $E(N_+(t_0))$ at any fixed t_0 .

Equation (15) implies that Good-Toulmin estimator [Good and Toulmin, 1956]

$$\hat{\psi}(t) = n_+(t_0) + \sum_{k=1}^{\infty} (-1)^{k+1} n_k(t_0) \left(\frac{t}{t_0} - 1 \right)^k$$

is an unbiased estimator of $\psi(t)$ under the framework. This estimator works well in interpolation (i.e. $0 \leq t \leq t_0$), and performs satisfactorily in short-term extrapolation when $t_0 < t \leq 2t_0$. The curve $\hat{\psi}(t)$ for $0 \leq t \leq t_0$ is known as the rarefaction curve where a more intuitive expression is $\hat{\psi}(t) = \sum_{k=1}^{\infty} n_k(t_0)(1 - (1 - t/t_0)^k)$ when $0 \leq t \leq t_0$ because each species with frequency k at time t_0 has probability $(1 - (1 - t/t_0)^k)$ to be observed before time t (similar expression appears in Arrhenius [1921] where time is replaced by area).

We can deduce estimator for the derivative of $\psi(t)$ from the rarefaction curve. For example,

$$\hat{\psi}^{(1)}(t) = \frac{1}{t_0} \sum_{k=1}^{\infty} k n_k(t_0) \left(1 - \frac{t}{t_0} \right)^{k-1}, \quad (17)$$

$$\hat{\psi}^{(2)}(t) = -\frac{1}{t_0^2} \sum_{k=2}^{\infty} k(k-1) n_k(t_0) \left(1 - \frac{t}{t_0} \right)^{k-2}, \quad (18)$$

and

$$\hat{\psi}^{(3)}(t) = \frac{1}{t_0^3} \sum_{k=3}^{\infty} k(k-1)(k-2) n_k(t_0) \left(1 - \frac{t}{t_0} \right)^{k-3}. \quad (19)$$

We use the above estimators only when $t \in [0, t_0]$ because interpolation is more reliable than extrapolation.

The above derivative estimators are useful. For example, a concave downward curve when we plot $1/\hat{\psi}^{(1)}(t)$ for $t \in [0, t_0]$ is an indication that $E(D) = \infty$ because if there is a linear function $b + ct$ with positive b and c such that $b + ct \geq 1/\psi^{(1)}(t)$ for all $t \geq 0$. Then

$$E(D) = \int_0^{\infty} \psi^{(1)}(x) dx \geq \int_0^{\infty} (b + cx)^{-1} dx = \infty.$$

5 Derivative Ratio

A way to study a SAD is to consider the probability ratio, $p_j(t)/p_{j+1}(t)$ for $j = 1, 2, \dots$. It is equivalent to examine $-\psi^{(j)}(t)/\psi^{(j+1)}(t)$ ($= tp_j(t)/[(j+1)p_{j+1}(t)]$), which we call

the j th derivative ratio. From (11) and the Cauchy-Schwarz inequality, for $j = 1, 2, \dots$ and $t \geq 0$

$$\psi^{(j)}(t)\psi^{(j+2)}(t) \geq (\psi^{(j+1)}(t))^2.$$

It deduces that j th derivative ratio is always a nondecreasing function of t . Denote the first derivative ratio by $\xi(t)$. A sufficient condition for $\xi(t)$ to associate with an ESAC is that it is a Bernstein function because $\psi^{(2)}(t)\xi(t) = -\psi^{(1)}(t)$ implies that

$$\sum_{i=0}^{k-2} \binom{k-2}{i} \psi^{(k-i)}(t)\xi^{(i)}(t) = -\psi^{(k-1)}(t), \quad (k \geq 2)$$

which by mathematical induction, leads to $(-1)^{k-1}\psi^{(k)}(t) \geq 0$ for $k \geq 1$ when we restrict to the solution with positive $\psi^{(1)}(t)$.

5.1 First Linear Derivative Ratio Family

The simplest nontrivial Bernstein function is the positive linear function in $[0, \infty)$. We call the family of ESACs with $\xi(t) = b + ct$, the first linear derivative ratio family, and denote it as LDR₁. Clearly $b \geq 0$. If $b = 0$, c must be larger than 1, otherwise $\psi(t)$ can be infinite for finite t as seen from (21). It is proved in Appendix B that under LDR₁,

$$\frac{p_j(t)p_{j+2}(t)}{p_{j+1}^2(t)} = \frac{(j+1)(jc+1)}{(j+2)((j-1)c+1)} \quad (j \geq 1). \quad (20)$$

Fixing $\psi^{(1)}(1) = a > 0$,

$$\psi(t) = \begin{cases} \frac{a(b+c)}{c-1} \left(\left(\frac{b+ct}{b+c} \right)^{1-1/c} - \left(\frac{b}{b+c} \right)^{1-1/c} \right) & (c \neq 0, 1), \\ ab \exp(1/b)(1 - \exp(-t/b)) & (c = 0), \\ a(b+1) \log(1 + (t/b)) & (c = 1). \end{cases} \quad (21)$$

Parameter a is a scale parameter. For $k = 1, 2, \dots$,

$$\psi^{(k)}(t) = \begin{cases} (-1)^{k+1} \frac{a(b+c)^{1-k} c^{k-1} \Gamma(1/c+k-1)}{\Gamma(1/c)} \left(\frac{b+ct}{b+c} \right)^{1-1/c-k} & (c > 0), \\ (-1)^{k+1} ab^{1-k} \exp((1-t)/b) & (c = 0). \end{cases}$$

From (13),

$$E(N_k(t)) = \begin{cases} \frac{a(b+c)^{1-k} c^{k-1} t^k \Gamma(1/c+k-1)}{k! \Gamma(1/c)} \left(\frac{b+ct}{b+c} \right)^{1-1/c-k} & (c > 0), \\ ab^{1-k} t^k \exp((1-t)/b)/k! & (c = 0). \end{cases}$$

It can be shown that $\nu(\{0\}) = 0$, and

$$\tilde{\nu}(d\lambda) = \begin{cases} \frac{a((b+c)/c)^{1/c} \lambda^{1/c-2}}{\Gamma(1/c)} \exp(-b\lambda/c) d\lambda & (c > 0), \\ ab \exp(1/b) \delta_{1/b}(d\lambda) & (c = 0), \end{cases} \quad (22)$$

where $\delta_{1/b}(A) = \mathbf{1}\{1/b \in A\}$ is the Dirac measure. The intensity function $\tilde{\nu}$ takes the form as a gamma distribution with extended shape parameter $1/c - 1$ for nonnegative c . Therefore, $p(t)$ is the Engen's extended negative binomial distribution [Engen, 1974] with support $\{1, 2, \dots\}$. Engen's extended negative binomial distribution also appears in the model studied by Zhou et al. [2017].

The expected total number of species is

$$E(D) = \lim_{t \rightarrow \infty} \psi(t) = \begin{cases} a(b+c)^{1/c} b^{1-1/c} (1-c)^{-1} & (0 < c < 1), \\ ab \exp(1/b) & (c = 0), \\ \infty & (c \geq 1). \end{cases}$$

If $\psi(t) \in \text{LDR}_1$, $E(D) = \infty$ if and only if $E(N_k(t))$ keeps increasing as t increases for any fixed k . When $E(D) < \infty$, $E(N_k(t))$ is unimodal with respect to t .

When $0 \leq c < 1$, $E(N_0(t))$ is finite. Define $p_0(t) = E(N_0(t))/E(N_+(t))$ (it is not a probability and can be larger than 1). It can be proved that when $0 \leq c < 1$, (20) remains to be true when $j = 0$. Therefore, when $0 \leq c < 1$,

$$E(N_0(t)) = \frac{p_1(t)^2 E(N_+(t))}{2(1-c)p_2(t)} = \frac{E^2(N_1(t))}{2(1-c)E(N_2(t))}. \quad (23)$$

Equation (23) portrays a relation among rare species, and is useful when the data for rare species follows LDR_1 with the c in (23) being the derivative of $\xi(t)$ regardless of the stochastic structure of the abundant species. An estimate of c can be found by solving (20) for c when $j = 1$ with all $p_j(t_0)$'s replaced by their relative frequency estimates. As theoretically $c \geq 0$, the estimate of c is $\hat{c}^* = \max(3n_1(t_0)n_3(t_0)/(2n_2^2(t_0)) - 1, 0)$. It is an estimate of c for the LDR_1 model for rare species because \hat{c}^* depends only on the counts of singletons, doubletons and tripletons. From (23), an estimator of $E(D)$ is

$$\hat{E}^*(D) = \begin{cases} n_+(t_0) + n_1^2(t_0)/[2(1-\hat{c}^*)n_2(t_0)] & \text{if } \hat{c}^* < 1 \\ \infty & \text{if } \hat{c}^* \geq 1 \end{cases} \quad (24)$$

This estimator is applicable when the data for rare species follows LDR_1 and all abundant species are seen in the study (thus their contribution to D has already been

included in $n_+(t_0)$). If $\hat{c}^* = 0$ (from (22), $c = 0$ corresponds to the case when all species have the same rate), it is the Chao1 estimator [Chao, 1984].

Family LDR_1 includes the following existing models. Most of them have simple form of $\psi^{(1)}(t)$ which facilitates easy graphical check.

- Case $c = 0$: Zero-truncated Poisson distribution for the SAD, negative exponential law for the ESAC.

When $c = 0$, $E(N_k(t)) = ab \exp(1/b)(t/b)^k \exp(-t/b)/k!$ is proportional to a zero-truncated Poisson distribution. It is the simplest SAD with all species having the same rate $1/b$. The ESAC is $\psi(t) = ab \exp(1/b)(1 - \exp(-t/b))$ which is the negative exponential law. A diagnostic graph specially designed for it is to plot $\log(\hat{\psi}^{(1)}(t))$ against $t \in [0, t_0]$ for $\hat{\psi}^{(1)}(t)$ defined in (17). If the model is correct, we should see a curve close to a straight line because $\log(\psi^{(1)}(t)) = 1/b + \log(a) - t/b$.

- Case $0 < c < 1$: Zero-truncated negative binomial distribution for the SAD.

When $0 < c < 1$, $\tilde{\nu}$ is proportional to a gamma probability measure, and $p(t)$ is the probability vector for the zero-truncated negative binomial distribution.

- Case $c = 1/2$: Geometric distribution for the SAD, hyperbola law for the ESAC.

A special value of c in $(0, 1)$ is $c = 1/2$. The $\tilde{\nu}$ is proportional to an exponential probability measure and $p(t)$ is a geometric probability vector. The ESAC is $\psi(t) = a(2b + 1)^2 t / (2b(t + 2b))$ which is the hyperbola law (also known as Michaelis-Menten equation and Monod model). A graph for this distribution is to plot $(\hat{\psi}^{(1)}(t))^{-1/2}$ as a function of $t \in [0, t_0]$. If geometric distribution fits the data, we should see an almost linear curve because $(\psi^{(1)}(t))^{-1/2} = (t + 2b)/(a^{1/2}(2b + 1))$.

- Case $c = 1$: Log-series distribution for the SAD, Kobayashi's logarithm law for the ESAC.

When $c = 1$, $E(N_k(t)) = a(b + 1)(t/(t + b))^k/k$ corresponding to the log-series distribution. The ESAC is $\psi(t) = a(b + 1) \log(1 + t/b)$ which was introduced in Kobayashi [1975] (see also Fisher et al. [1943] and May [1975]). A graph for the log-series distribution is to draw $1/\hat{\psi}^{(1)}(t)$ as a function of $t \in [0, t_0]$. If the

model is good, the curve should be close to a straight line because $1/\psi^{(1)}(t) = (b+t)/(a(b+1))$.

- Case $b = 0$ (it implies $c > 1$): Power law for the ESAC.

When $c > 1$ and $b = 0$, $\psi(t) = act^{1-1/c}/(c-1)$ is the power law. For $k = 1, 2, \dots$,

$$p_k(t) = \frac{(c-1)\Gamma(1/c+k-1)}{k!c\Gamma(1/c)}, \quad (25)$$

which does not depend on t . Power law is the only ESAC having this property (proof is given in Appendix C). At any time, the probability of singleton is $(c-1)/c$, the probability of doubleton is $(c-1)/(2c^2)$ and so on. The probability vector in (25) also appears in Zhou et al. [2017]. From (21), when $c > 1$ and t is large, $\psi(t)$ in LDR_1 behaves like a power law. When c approaches infinity, $\psi(t)$ tends to at which corresponds to a population containing only zero-probability species. A graph to check the power law is to plot $\log(\hat{\psi}^{(1)}(t))$ against $\log(t)$. The curve should be approximately linear because $\log(\psi^{(1)}(t)) = \log(a) - c^{-1}\log(t)$. We call this plot, $\log(D)$ - \log plot.

Currently a standard diagnostic plot for power law is the log-log plot which plots $\log(\hat{\psi}(t))$ against $\log(t)$. An approximate linear curve in the plot is an indication that power law fits the data. As $d\log(\psi(t))/d\log(t) = p_1(t)$, log-log plot detects whether $p_1(t)$ is a constant. On the other hand, $\log(D)$ -log plot checks whether $p_2(t)/p_1(t)$ is a constant because $d\log(\psi^{(1)}(t))/d\log(t) = -2p_2(t)/p_1(t)$. Log(D)-log plot is more sensitive to discrepancies of the power law because $p_1(t)$ changes very slowly for many SADs. It is well-known in species-area relationship studies that the curve in log-log plot is approximately linear for various dissimilar SADs [Preston, 1960, 1962, May, 1975, Martin and Goldenfield, 2006].

5.2 Second Linear Derivative Ratio Family

We extend the first linear derivative ratio family to j th linear derivative ratio family, which we denote as LDR_j . A $\psi(t)$ belongs to LDR_j if $-\psi^{(j)}(t)/\psi^{(j+1)}(t)$ is a linear function of t . We prove in Appendix D that $\text{LDR}_2 = \text{LDR}_3 = \dots$. Thus we only need to consider LDR_2 .

An ESAC, $\psi(t)$ belongs to LDR_2 if $-\psi^{(2)}(t)/\psi^{(3)}(t) = \tilde{b} + \tilde{c}t$. If we fix $\psi^{(2)}(1) = -\tilde{a}$ and $\psi^{(1)}(1) = \tilde{r} + \tilde{a}(\tilde{b} + \tilde{c})/(1 - \tilde{c})$, it can be proved that

$$\text{LDR}_2(t \mid \tilde{a}, \tilde{b}, \tilde{c}, \tilde{r}) = \tilde{r}t + \text{LDR}_1\left(t \mid \tilde{a}(\tilde{b} + \tilde{c})/(1 - \tilde{c}), \tilde{b}/(1 - \tilde{c}), \tilde{c}/(1 - \tilde{c})\right),$$

where $\text{LDR}_2(t \mid \tilde{a}, \tilde{b}, \tilde{c}, \tilde{r})$ denotes the $\psi(t)$ for LDR_2 , and $\text{LDR}_1(t \mid a, b, c)$ denotes the $\psi(t)$ for LDR_1 . We have $\tilde{a} > 0$, $\tilde{b} \geq 0$, $0 \leq \tilde{c} < 1$, and $\tilde{r} \geq 0$. If $\tilde{b} = 0$, then $1/2 < \tilde{c} < 1$, otherwise $\psi(t)$ will be infinite for finite t . The linear component $\tilde{r}t$ in $\text{LDR}_2(t \mid \tilde{a}, \tilde{b}, \tilde{c}, \tilde{r})$ is the part for the zero-probability species. Therefore, LDR_2 is simply a mixture of zero-probability species and LDR_1 .

5.3 D1/D2 and D2/D3 Plots

An advantage of LDR_1 is that it has a simple diagnostic plot: Draw $\hat{\xi}(t) = -\hat{\psi}^{(1)}(t)/\hat{\psi}^{(2)}(t)$ as a function of $t \in [0, t_0]$ for $\hat{\psi}^{(1)}(t)$ and $\hat{\psi}^{(2)}(t)$ defined in (17) and (18) respectively. If the curve in the plot is almost linear, LDR_1 is an appropriate model and approximate value of b and c can be obtained from a fitted linear function to the curve. We call the plot, D1/D2 plot. Similarly, to investigate how well LDR_2 fits a data, we can plot the function $-\hat{\psi}^{(2)}(t)/\hat{\psi}^{(3)}(t)$ for $t \in [0, t_0]$ where $\hat{\psi}^{(2)}(t)$ and $\hat{\psi}^{(3)}(t)$ are defined in (18) and (19) respectively. We call the plot, D2/D3 plot. Theoretically, the true curve in both D1/D2 and D2/D3 plots must be nondecreasing, but their estimates may not have this property.

By delta method,

$$\text{Var}(\hat{\xi}(t)) \approx \frac{\text{Var}(\hat{\psi}^{(1)}(t))}{E^2(\hat{\psi}^{(2)}(t))} + \frac{E^2(\hat{\psi}^{(1)}(t))\text{Var}(\hat{\psi}^{(2)}(t))}{E^4(\hat{\psi}^{(2)}(t))} - \frac{2E(\hat{\psi}^{(1)}(t))\text{Cov}(\hat{\psi}^{(1)}(t), \hat{\psi}^{(2)}(t))}{E^3(\hat{\psi}^{(2)}(t))}.$$

We can approximate $\text{Var}(\hat{\xi}(t))$ by

$$\widehat{\text{Var}}(\hat{\xi}(t)) = \frac{\widehat{\text{Var}}(\hat{\psi}^{(1)}(t))}{\hat{\psi}^{(2)2}(t)} + \frac{\hat{\psi}^{(1)2}(t)\widehat{\text{Var}}(\hat{\psi}^{(2)}(t))}{\hat{\psi}^{(2)4}(t)} - \frac{2\hat{\psi}^{(1)}(t)\widehat{\text{Cov}}(\hat{\psi}^{(1)}(t), \hat{\psi}^{(2)}(t))}{\hat{\psi}^{(2)3}(t)},$$

where

$$\begin{aligned}\widehat{\text{Var}}(\hat{\psi}^{(1)}(t)) &= \sum_{k=1}^{\infty} k^2 n_k(t_0) (1 - t/t_0)^{2k-2}, \\ \widehat{\text{Var}}(\hat{\psi}^{(2)}(t)) &= \sum_{k=2}^{\infty} k^2 (k-1)^2 n_k(t_0) (1 - t/t_0)^{2k-4},\end{aligned}$$

and

$$\widehat{Cov}(\hat{\psi}^{(1)}(t), \hat{\psi}^{(2)}(t)) = \sum_{k=2}^{\infty} k^2(k-1)n_k(t_0)(1-t/t_0)^{2k-3}.$$

We use

$$\hat{\xi}(t) \pm 1.96\sqrt{\widehat{Var}(\hat{\xi}(t))}$$

as an approximate 95% pointwise confidence band for the D1/D2 plot. Similar confidence band can be constructed for D2/D3 plot.

Let $\xi_1(t)$ and $\xi_2(t)$ be the first derivative ratio of two ESACs, $\psi_1(t)$ and $\psi_2(t)$ respectively. If $\xi_1(t) \geq \xi_2(t)$ for all $t \geq t^* > 0$, then $\log(\psi_1^{(1)}(t)/\psi_2^{(1)}(t))$ is a nondecreasing function of t . Thus $(\psi_1(t) - \psi_1(t^*))/\psi_2^{(1)}(t^*) \geq (\psi_2(t) - \psi_2(t^*))/\psi_2^{(1)}(t^*)$ whenever $t > t^*$. If we can judge from a D1/D2 plot that $\xi(t)$ is bounded from below by a linear function with slope 1 (it is $\xi(t)$ for a log-series distribution), then the above inequality implies that $E(D)$ is infinite. On the other hand, if $\xi(t)$ is bounded from above by a linear function with slope less than 1 (it corresponds to a $\xi(t)$ with finite $E(D)$), $E(D)$ is finite.

6 An Extended Family of LDR₁

A very common observation in species abundance studies is that there are many rare species and only a few highly abundant species. Abundant species are usually seen early in the survey and affect mainly the front part of $\xi(t)$. Therefore, the rear part of $\xi(t)$ reflects largely the stochastic structure of rare species. If linear function does not fit the whole $\xi(t)$, it may still fit the rear part. In this case, LDR₁ can be used to fit only the data for the rare species. One method is to fit the rear part of $\xi(t)$ by a straight line passing through the end point $\hat{\xi}(t_0)$ with slope $\hat{\xi}^{(1)}(t_0)$. It can be checked that this method gives an estimate of $E(D)$ that coincides with $E^*(D)$ in (24) when $\hat{\xi}^{(1)}(t_0) \geq 0$. If parametric approach is desired, we want a generalization of LDR₁ such that the rear part of $\xi(t)$ is always approximately linear. A Bernstein function which is asymptotically linear is $\xi(t) = 1/[c_1/(t+b_1) + c_2/(t+b_2)]$ for nonnegative constants $b_1 < b_2$, c_1 and c_2 . When $c_2 = 0$ (or $c_1 = 0$), it reduces to LDR₁. In all cases, it is approximately linear with slope $1/(c_1 + c_2)$ when t is large. It can be proved by

mathematical induction that for $k \geq 1$,

$$k(k-1+c_1+c_2)\psi^{(k)}(t)+[c_1t+b_2c_1+c_2t+b_1c_2+k(2t+b_1+b_2)]\psi^{(k+1)}(t)+(t+b_1)(t+b_2)\psi^{(k+2)}(t)=0.$$

Given $a = \psi^{(1)}(t_0)$ which is a scale parameter, and the parameters b_1 , b_2 , c_1 and c_2 , we can find $\psi^{(2)}(t_0) = -\psi^{(1)}(t_0)/\xi(t_0)$ and then apply the above recurrence relation for $t = t_0$ to compute all necessary $\psi^{(k)}(t_0)$ in (14). The ESAC is

$$\psi(t) = a(t_0 + b_1)^{c_1}(t_0 + b_2)^{c_2} \int_0^t (x + b_1)^{-c_1}(x + b_2)^{-c_2} dx,$$

which can be computed numerically. Quantity $E(D) = \lim_{t \rightarrow \infty} \psi(t)$ is finite if and only if $c_1 + c_2 > 1$. We denote the model with this rational polynomial form of $\xi(t)$ by RDR_1 .

7 Examples

Four real FoF data are presented in Table 1. Nonparametric analysis of the data can be found in Böhning and Schön [2005], Lijoi, Mena, and Prünster [2007], Wang [2010], Chee and Wang [2016] and Chiu and Chao [2016]. Except for the third dataset, $\hat{E}^*(D) = \infty$. In this section, we fit the data using the parametric models in Sections 5 and 6. The significance level of the tests is fixed to 5%.

The first data is the swine feces data which appeared and was analyzed in Chiu and Chao [2016]. It is for the pooled contig spectra from seven non-medicated swine feces. The large $n_1(t_0)$ relative to other frequencies is viewed as a signal for sequencing errors. Chiu and Chao [2016] proposed a nonparametric estimate of the singleton count basing on the other counts, and the difference of this estimate and the observed singleton count is interpreted as outcome of missequencing. An implicit assumption of this approach is that sequencing errors inflate only the singleton count, and all other frequency counts are unaffected. It is equivalent to claim that sequencing errors create solely “zero-probability species”.

To investigate whether zero-probability species really exist, we draw the D1/D2 and D2/D3 plots with 95% pointwise confidence bands for the data in panels (a) and (b) respectively in Figure 2. The approximate linear curve in both plots indicates that both LDR_1 and LDR_2 are reasonable models. The heavy dashed lines in panels (a)

Table 1: Four real FoF data (the values \hat{a} , \hat{b} and \hat{c} are MLE under LDR_1 model)

(i) Swine feces data ($\hat{a} = 8027.6, \hat{b} = 2.878, \hat{c} = 3.963$)																	
k	1	2	3	4	5	6	7	8	9	10	11						
$n_k(t_0)$	8025	605	129	41	16	8	4	2	1	1	1						
(ii) Microbial species data ($\hat{a} = 383.6, \hat{b} = 0.171, \hat{c} = 3.155$)																	
k	1	2	3	4	5	6	7	9	11	13	14	16	21	27	32	43	
$n_k(t_0)$	381	65	23	18	4	5	3	1	4	3	2	1	1	1	1	1	
(iii) Accident data ($\hat{a} = 1320.3, \hat{b} = 1.817, \hat{c} = 1.115$)																	
k	1	2	3	4	5	6	7										
$n_k(t_0)$	1317	239	42	14	4	4	1										
(iv) Tomato flowers data ($\hat{a} = 1444.3, \hat{b} = 0.739, \hat{c} = 2.578$)																	
k	1	2	3	4	5	6	7	8	9	10	11	12	13	14	16	23	27
$n_k(t_0)$	1434	253	71	33	11	6	2	3	1	2	2	1	1	1	2	1	1

and (b) are the fitted lines under LDR_1 . The fitted line is close to the curve in D1/D2 plot, but is not so in the D2/D3 plot. As the dashed line lies inside the confidence bands in panel (b), the disagreement between the singleton count and other counts is not strong enough to reject that they come from the fitted LDR_1 . The Pearson's chi-square test statistic after grouping all cells with expected frequency less than 5 is 4.325 with 4 degrees of freedom. The estimated $E(N_1(t_0))$ under this LDR_1 is 8027.6 which is marginally larger than $n_1(t_0)$. As $\hat{E}(N_1(t_0)) > n_1(t_0)$, the MLE of $\nu(0)$ under LDR_2 should be zero, and LDR_1 is our selected model. There is no significant evidence for the existence of zero-probability species. As the estimated c for LDR_1 is larger than 1, the estimated $E(D)$ is infinite.

The second data is the microbial species data which was studied in Wang [2010] and Chee and Wang [2016]. The D1/D2 plot of the data is displayed in panel (c) in Figure 2. The curve looks quite linear. The heavy dashed line is the fitted line under LDR_1 . The MLE of c is 3.155 meaning that the estimated $E(D)$ is infinite. The heavy solid line (indistinguishable with $\hat{\xi}(t)$ in D1/D2 plot) is the fitted curve under RDR_1 .

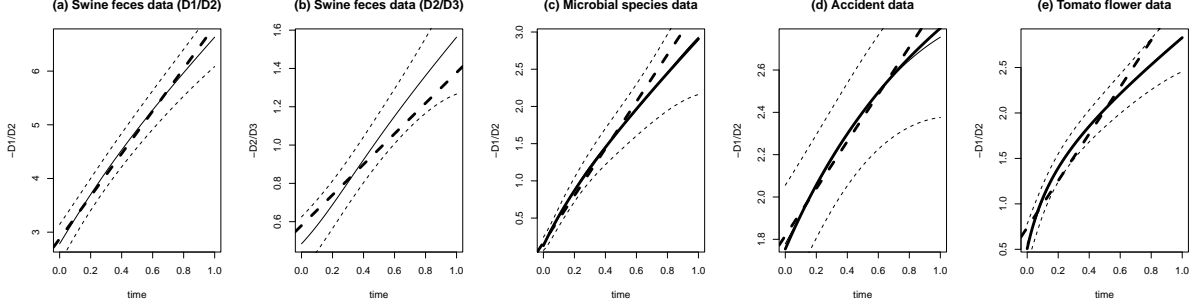


Figure 2: $D1/D2$ and $D2/D3$ plots for the data. The light solid curves are the $D1/D2$ or $D2/D3$ curve. The light dashed curves are the 95% pointwise confidence bands. The heavy dashed lines are the fitted lines under LDR_1 . The heavy solid curves in panels (c) - (e) are the fitted curves under RDR_1 . The heavy and light solid curves are so close that it is hard to distinguish the twos in the plots except in the right end in panel (d).

The likelihood-ratio test shows that RDR_1 model is not significantly better than LDR_1 model.

The third data come from 9461 accident insurance policies issued by an insurance company. It was used in Böhning and Schön [2005], Wang [2010] and Chee and Wang [2016]. The species corresponds to the policies and the frequency count to the number of claims during a particular year. The $\hat{\xi}(t)$ in the $D1/D2$ plot for the accident data in panel (d) is quite linear. The p-value for the Pearson chi-square test is 0.0979. The estimate of c is 1.1146, and an approximate 95% confidence interval for c is $[0.7499, 1.5485]$ which overlaps with $[0, 1)$. It means that $\hat{E}(D) = \infty$, but the hypothesis that $E(D)$ is finite is not rejected. The heavy solid curve in panel (d) is the fitted curve under RDR_1 . Model RDR_1 is not statistically better than LDR_1 . The MLE of $E(D)$ under RDR_1 is 6353. It is less than the true value $D = 9461$, and is comparable to the nonparametric estimates presented in Chee and Wang [2016] which ranges from 4016 to 7374. For this data, $\hat{c}^* = 0.4525$ and $\hat{E}^*(D) = 8249.2$ which is closer to the true value.

The last data come from a CDNA library of the expressed sequence tags of tomato flowers. It was studied in Böhning and Schön [2005] and Lijoi, Mena, and Prünster

[2007]. The D1/D2 plot in panel (e) shows that LDR_1 model does not fit the data well. The curve looks like a Bernstein function. An RDR_1 model is fitted and the fitted curve is shown in the plot by a heavy solid curve. It almost coincides with the D1/D2 curve. The model fits the data well (Pearson's chi-square statistic after grouping all cells with expected frequency less than 5 is 1.470 with 2 degrees of freedom). It is significantly better than LDR_1 model. The MLE of b_1 , b_2 , c_1 and c_2 are 0.050, 1.451, 0.074 and 0.693 respectively. As $\hat{c}_1 + \hat{c}_2 = 0.767 < 1$, the estimated $E(D)$ is infinity.

8 Sampling Design

In the preceding sections, we consider a simple stopping rule for the survey – stop the study at a predesignated time t_0 . This design has two weaknesses. First, it does not control directly the amount of information collected because the size of our data is a random variable, the distribution of which we may have limited knowledge before the study. Second, it collects all available information within the survey period, instead of focusing only on the most valuable information in order to save labor.

For the first weakness, we may stop the survey as soon as a fixed number of species are recorded. To ensure termination of study with probability one, we set an upper bound for the study period which is the time at which the data collection process must end. The stopping rule principle states that the likelihood function is the same irrespective of the stopping rule [Raiffa and Schlaifer, 1961, Berger and Berry, 1988]. By this principle, the likelihood function of the proposed design is identical to the one with the actual stopping time pretended to be fixed instead of random. In other words, the log-likelihood function in (9) can be used with t_0 being the realization of the random stopping time.

For the second weakness, we can halt recording a species as soon as its frequency reaches a fixed positive integer, say ρ . Thus the observation period for each species varies. The period is short for abundant species, and long for rare species. Again, we need to set an upper bound for the study period, say t_0 for all species. We call this design, the ρ -appearance design. This design places more emphasis on rare species than abundant species which is in line with the common understanding that information

about the rare species is critical in biodiversity estimation. In bird survey, species can be identified by distant sightings or short bursts of song. Stop recording abundant species early helps the researcher concentrating more on the rare species. When $\rho = \infty$, we obtain $\tilde{n}(t_0)$. When $\rho = 1$, we record only the first appearance-time of each seen species. It is exactly the information available in the empirical SAC.

In this design, we collect value (R_i, J_i) for each seen species, say species i . Species i has observed frequency J_i at time R_i . Clearly $R_i \leq t_0$ for all i . Suppose we call the recorded species with frequency less than ρ as rare species, and all other recorded species as abundant species. For rare species, $(R_i, J_i) = (t_0, J_i)$ where J_i is the frequency of species i in the whole study period $[0, t_0]$. No information is lost for rare species. For abundant species, $(R_i, J_i) = (R_i, \rho)$ where R_i is the appearance time of the ρ th individual of species i . We call R_i , the ρ -appearance time of species i . We do not know the actual frequency of abundant species in $[0, t_0]$. The values $n_1(t_0), \dots, n_{\rho-1}(t_0)$ and $n_+(t_0)$ are still available. It is proved in Appendix E that the log-likelihood function given a realization of $\{(R_i, J_i)\}_i$, say $\{(r_i, j_i)\}_i$ is

$$\log(\mathcal{L}(\psi \mid \{r_i, j_i\}_i)) = -\psi(t_0) + \sum_{j=1}^{\rho-1} n_j(t_0) \log(|\psi^{(j)}(t_0)|) + \sum_{r_i < t_0} \log(|\psi^{(\rho)}(r_i)|). \quad (26)$$

The above log-likelihood function can also be obtained from the stopping rule principle. As the likelihood function depends only on the data, not the stopping rule, the likelihood can be found by pretending that r_i is fixed to the observed value and j_i is random for each i . Equation (26) is the log-likelihood function of this latter artificial design (see (27) for the relation between $\psi^{(\rho)}(r)$ and the intensity function of the ρ -appearance time). A computational advantage of ρ -appearance design is that the log-likelihood function is simple even for complicated $\psi(t)$ because it depends only on the leading ρ derivatives of $\psi(t)$.

By the displacement theorem of Poisson process [Kingman, 1993], the ρ -appearance times form a Poisson process with intensity function

$$f_\rho(r) = \int \frac{\lambda^\rho r^{\rho-1} \exp(-\lambda r)}{(\rho-1)!} \tilde{\nu}(d\lambda) = \int \frac{(\lambda r)^{\rho-1} \exp(-\lambda r)}{(\rho-1)!} \nu(d\lambda) = \frac{r^{\rho-1}}{(\rho-1)!} (-1)^{\rho-1} \psi^{(\rho)}(r). \quad (27)$$

From (13), another expression for $f_\rho(r)$ is $f_\rho(r) = \rho E(N_\rho(r))/r$. Equation (27) give another interpretation of $\psi^{(k)}(t)$. For example, $\psi^{(1)}(r)$ is the intensity function of the

1-appearance times, and $r|\psi^{(2)}(r)|$ is the intensity function of the 2-appearance times.

9 Inference on Empirical Species Accumulation Curve

Suppose we only observe the empirical SAC, $n_+(t)$ for $t \in [0, t_0]$, or equivalently, the 1-appearance times of all seen species (i.e., the case $\rho = 1$ in Section 8). Let $r_1, \dots, r_{n_+(t_0)}$ be the 1-appearance times observed in $[0, t_0]$. From Section 8, the 1-appearance times of the recorded species form a Poisson process with intensity function $\psi^{(1)}(t)$. Thus $n_+(t_0)$ is a realization of a $\text{Poisson}(\psi(t_0))$ distribution. Given $n_+(t_0)$, $\{r_1, \dots, r_{n_+(t_0)}\}$ is a random sample of size $n_+(t_0)$ from the distribution function $\psi(t)/\psi(t_0)$. From (26), the log-likelihood function is

$$\log(\mathcal{L}(\psi \mid \{r_i\})) = \sum_{i=1}^{n_+(t_0)} \log(\psi^{(1)}(r_i)) - \psi(t_0).$$

If $\psi(t)$ has a free scale parameter, MLE of $\psi(t_0)$ is $n_+(t_0)$. The MLE of $\psi(t)$ for power law has a simple closed form $n_+(t_0)(t/t_0)^z$, where $z = \min\{n_+(t_0)/\sum_i \log(t_0/r_i), 1\}$.

Given a parametric form of $\psi(t)$, a traditional approach is to fit it to the empirical SAC by linear or non-linear least-squares method. Two differences between the MLE approach and the curve-fitting method are noteworthy. First, the MLE of $\psi(t_0)$ is equal to $n_+(t_0)$ whenever $\psi(t)$ has a free scale parameter, and it is not the case in the curve-fitting approach. As a result, the curve-fitting method may give unreasonable estimate of the total number of seen species when the current survey is extended because the estimate may be smaller than $n_+(t_0)$. Second, the MLE method fits the 1-appearance times to its density function $\psi^{(1)}(t)/\psi(t_0)$, while the curve-fitting method fits a distribution function to the empirical distribution function directly. The curve-fitting methods do not take the interdependence among the points in the empirical SAC into consideration. Since such interdependence is present in species-time curves and Type I species-area curves [Scheiner, 2003], the curve-fitting approach is theoretically flawed.

In certain situations, only the values of the empirical SAC at a finite set of points are available. For example, only the cumulative number of species observed after day 1, day 2, and so on are recorded. Suppose the observed $N_+(\ell_i)$ is $n_+(\ell_i)$ for $i = 1, \dots, m$

with $0 = \ell_0 < \ell_1 < \dots < \ell_m = t_0$. The log-likelihood function is

$$\log(\mathcal{L}(\theta \mid \{n_+(\ell_i)\})) = \sum_{i=1}^m (n_+(\ell_i) - n_+(\ell_{i-1})) \log(\psi(\ell_i|\theta) - \psi(\ell_{i-1}|\theta)) - n_+(t_0) \log(\psi(t_0|\theta)).$$

In the simulation study in Appendix G, MLE always has smaller root mean squared relative error in extrapolation when compared to the curve-fitting method.

The distribution function of the 1-appearance times in time interval $[0, t_0]$ is $\psi(t)/\psi(t_0)$. This fact holds generally and the only restriction on $\psi(t)$ is that $\psi(t)$ is nondecreasing and $\psi(0) = 0$. Apart from the ESACs under the mixed Poisson partition process, $\psi(t)$ can be sigmoid functions such as the cumulative Weibull function and the cumulative beta-P function. If we assume that the 1-appearance times are independent, we can perform maximum likelihood inference conditional on $n_+(t_0)$ when a parametric form of $\psi(t)$ is given. Full maximum likelihood calculation is possible when distribution assumption is made for $N_+(t_0)$. As the empirical SAC is proportional to the empirical distribution function of the 1-appearance times, statistical tools for empirical distribution function can be applied. For example we can apply the Dvoretzky-Kiefer-Wolfowitz inequality to construct confidence bands for the distribution function $\psi(t)/\psi(t_0)$.

10 Conclusion

The contributions of this paper are summarized as follows.

First, we introduce a general framework, called the mixed Poisson partition process which models the observed frequencies for all species along the time axis. The expected total number of species in the community as well as the expected number of individuals seen in any finite time interval can be finite or infinite. The model allows infinite number of species with zero detection probability. Parametric model can be defined by defining functional form for ν , $p(t)$, $\psi(t)$, $\psi^{(1)}(t)$ or $\xi(t)$. Each of them focuses on different aspects of the framework.

Second, we introduce a family of ESAC, LDR_1 which accompanies a simple diagnostic plot, D1/D2 plot. We propose two extensions of LDR_1 : (i) LDR_2 which includes zero-probability species, and (ii) RDR_1 which approximates LDR_1 when t is large. We also suggest a handy estimator $\hat{E}^*(D)$ which is useful when the rare species behaves like LDR_1 .

Third, we consider sampling design other than fixing the study period. A simple alternative is to fix the number of observed species. The ρ -appearance design puts more effort on rare species than abundant species. A simple example in Appendix F shows that the loss in information is marked when $\rho = 1$, and minor when $\rho = 4$.

Fourth, when only the empirical SAC is available, we show how MLE approach can be taken, and explain why MLE outperforms the traditional curve-fitting method.

Appendix A: Equivalent definition of the mixed Poisson partition process

The following alternative equivalent definition unifies the three steps in the definition into one.

Definition: (Equivalent definition of mixed Poisson partition process) A mixed Poisson partition process G is characterized by a species intensity measure ν , which is a measure over $\mathbb{R}_{\geq 0}$ satisfying $\int_0^\infty \min\{1, \lambda^{-1}\} \nu(d\lambda) < \infty$. Define $\dot{\nu}$ to be a measure over $\mathbb{R}_{\geq 0}^2$ by

$$\dot{\nu}(A) = \int \int_0^\infty \mathbf{1}\{(\lambda, t) \in A\} e^{-\lambda t} dt \cdot \nu(d\lambda)$$

for any measurable set $A \subseteq \mathbb{R}_{\geq 0}^2$ where $\mathbf{1}\{\cdot\}$ is the indicator function. Generate $(\lambda_1, t_1), (\lambda_2, t_2), \dots$ (a finite or countably infinite sequence) according to a Poisson process with intensity measure $\dot{\nu}$. For each simulated (λ_i, t_i) , we generate η_i (independently across i) according to a Poisson process with rate λ_i , conditioned on the event that the first point is at time t_i . (That is, it contains the point t_i together with a Poisson process starting at time t_i . If $\lambda_i = 0$, then η_i contains only one point t_i .) Finally, we take $G = \{\eta_1, \eta_2, \dots\}$.

This definition models the species that will eventually be observed in the study. The first appearance time for each of such species (i.e. the first point of each η_i) is explicitly included in the definition of $\dot{\nu}$.

The equivalence between the two definitions is a direct consequence of the marking theorem of Poisson process [Kingman, 1993]. Consider the joint process $\{(\lambda_i, t_i)\}$ for $\lambda > 0$, where t_i is the first point of η_i . By the marking theorem, this process is a Poisson process with intensity measure $\lambda e^{-\lambda t} \tilde{\nu} = e^{-\lambda t} \mathbf{1}\{\lambda > 0\} \nu$ (we write $f(\lambda, t) \nu$ for the measure $A \mapsto \int \int_0^\infty \mathbf{1}\{(\lambda, t) \in A\} f(\lambda, t) \nu(d\lambda)$). Since η_0 is a Poisson process with rate $\nu(\{0\})$, its contribution to the process $\{(\lambda_i, t_i)\}$ has an intensity measure

$\mathbf{1}\{\lambda = 0\}\nu$. By the superposition property of Poisson process, the overall intensity measure of the $\{(\lambda_i, t_i)\}$ process is $e^{-\lambda t}\mathbf{1}\{\lambda > 0\}\nu + \mathbf{1}\{\lambda = 0\}\nu = e^{-\lambda t}\nu$.

Appendix B: Proof of Equation (20)

For positive integer j , $\text{LDR}_j \subseteq \text{LDR}_{j+1}$ holds because $-\psi^{(j)}(t) = (b + ct)\psi^{(j+1)}(t)$ implies

$$-\psi^{(j+1)}(t) = c\psi^{(j+1)}(t) + (b + ct)\psi^{(j+2)}(t). \quad (28)$$

Therefore

$$\text{LDR}_1 \subset \text{LDR}_2 \subset \dots$$

Suppose $\psi(t) \in \text{LDR}_1$. Then $\psi(t) \in \text{LDR}_j$ for all $j \geq 1$. Write $-\psi^{(j)}(t)/\psi^{(j+1)}(t) = b_j + c_j t$. From (28), $c_{j+1} = c_j/(c_j + 1)$. It implies that $c_j = c_1/((j-1)c_1 + 1)$ for $j \geq 1$. Furthermore,

$$c_j = \frac{d(-\psi^{(j)}(t)/\psi^{(j+1)}(t))}{dt} = \frac{\psi^{(j)}(t)\psi^{(j+2)}(t)}{\psi^{(j+1)2}(t)} - 1 = \frac{(j+2)p_j(t)p_{j+2}(t)}{(j+1)p_{j+1}^2(t)} - 1.$$

Thus

$$\frac{p_j(t)p_{j+2}(t)}{p_{j+1}^2(t)} = \frac{(j+1)c_j}{j+2} = \frac{(j+1)c_1}{(j+2)((j-1)c_1 + 1)}.$$

Equation (20) follows as $c = c_1$.

Appendix C: Proof of the fact that power law is the only law with time-invariant species abundance distribution

Suppose $p(t) = p = (p_1, p_2, \dots)$ which does not depend on t . For $k = 1, 2, \dots$,

$$p_k\psi(t) = E(N_k(t)) = \int \frac{\exp(-\lambda t)\lambda^{k-1}t^k}{k!}\nu(d\lambda).$$

Therefore, for any y ,

$$\left(\sum_{k=1}^{\infty} p_k(1-y)^k\right)\psi(t) = \int \frac{\exp(-\lambda t)}{\lambda} \sum_{k=1}^{\infty} \frac{((1-y)\lambda t)^k}{k!}\nu(d\lambda) = \psi(t) - \psi(yt).$$

It follows that

$$\psi(yt) = \psi(t) \left(1 - \sum_{k=1}^{\infty} p_k(1-y)^k\right).$$

Take logarithm on both sides, take derivative with respect to t , and then set $t = 1$. We have

$$y\psi^{(1)}(y) = \frac{\psi^{(1)}(1)\psi(y)}{\psi(1)}.$$

The solution of the above differential equation is $\psi(y) = \psi(1)y^{\psi^{(1)}(1)/\psi(1)}$ which is the power law. Hence the power law is the only law with $p(t)$ independent on t .

Appendix D: Proof of $\text{LDR}_2 = \text{LDR}_3 = \dots$

In Appendix B, we have shown that $\text{LDR}_1 \subseteq \text{LDR}_2 \subseteq \dots$. For any ESAC $\psi(t)$, define $\phi(t) = \psi^{(1)}(0) - \psi^{(1)}(t)$. Clearly for $j = 1, 2, \dots$

$$\phi(t) \in \text{LDR}_j \text{ if and only if } \psi(t) \in \text{LDR}_{j+1}. \quad (29)$$

Suppose $\psi(t) \in \text{LDR}_3$, say $-\psi^{(3)}(t)/\psi^{(4)}(t) = \tilde{b} + \tilde{c}t$. Then $\phi(t) \in \text{LDR}_2$ and $-\phi^{(2)}(t)/\phi^{(3)}(t) = \tilde{b} + \tilde{c}t$. From the result in Section 5.2 in the paper,

$$\phi(t) = \tilde{r}t + \text{LDR}_1(t \mid \tilde{a}(\tilde{b} + \tilde{c})/(1 - \tilde{c}), \tilde{b}/(1 - \tilde{c}), \tilde{c}/(1 - \tilde{c})), \quad (30)$$

for $0 \leq \tilde{c} < 1$ and $\tilde{r} \geq 0$. Thus the general form of $\psi(t)$ which relates to the integration of $-\phi(t)$ has a term $-\tilde{r}t^2/2$. As $\psi(t)$ is a Bernstein function, the power of t cannot be larger than one. It implies that \tilde{r} must be zero. From (30), $\phi(t) \in \text{LDR}_1$. From (29), $\psi \in \text{LDR}_2$. It proves $\text{LDR}_3 = \text{LDR}_2$. Suppose $\text{LDR}_{j+1} = \text{LDR}_j$ for a $j \geq 2$. Let $\psi(t) \in \text{LDR}_{j+2}$. From (29), $\phi(t) \in \text{LDR}_{j+1} = \text{LDR}_j$. From (29), $\psi(t) \in \text{LDR}_{j+1}$. Thus $\text{LDR}_{j+2} = \text{LDR}_{j+1}$. The result follows by mathematical induction.

Appendix E: Direct proof of the log-likelihood function for ρ -appearance design

For a species with rate λ , the probability function of J is

$$P(J = j \mid \lambda) = \begin{cases} \frac{(\lambda t_0)^j e^{-\lambda t_0}}{j!} & (j < \rho) \\ \sum_{k=\rho}^{\infty} \frac{(\lambda t_0)^k e^{-\lambda t_0}}{k!} & (j = \rho). \end{cases} \quad (31)$$

Since the time of the ρ th individual follows Erlang(ρ, λ) distribution,

$$P(R \in [r, r + dr), J = \rho \mid \lambda) = \frac{\lambda^\rho r^{\rho-1} e^{-\lambda r}}{(\rho - 1)!} dr. \quad (32)$$

By (31) and (32), the joint probability density function of the observations $\{(R_i, J_i)\}_{i \leq n_+(t_0)}$ given ν is proportional to

$$e^{-\psi(t_0)} \left(\prod_{i: j_i < \rho} \int \frac{\lambda^{j_i-1} t_0^{j_i} e^{-\lambda t_0}}{j_i!} \nu(d\lambda) \right) \left(\prod_{i: j_i = \rho} \int \frac{\lambda^{\rho-1} r_i^{\rho-1} e^{-\lambda r_i}}{(\rho - 1)!} \nu(d\lambda) \right).$$

Therefore, the log-likelihood function is

$$\log(\mathcal{L}(\nu \mid \{r_i, j_i\}_i)) = -\psi(t_0) + \sum_{j=1}^{\rho-1} n_j(t_0) \log(|\psi^{(j)}(t_0)|) + \sum_{r_i < t_0} \log(|\psi^{(\rho)}(r_i)|).$$

Appendix F: Small simulation experiment on the loss of information of the ρ -appearance design

Consider the bird abundance data for the Wisconsin route of the North American Breeding Bird Survey for 1995. The data was studied in Norris and Pollock [1998] where a mixture of five Poisson models was fitted. The data, $(n_1(t_0), \dots, n_{54}(t_0))$ is $(11, 12, 10, 6, 2, 5, 1, 3, 2, 4, 0, 1, 1, 1, 2, 1, 0, 2, 0, 0, 0, 0, 0, 0, 1, 0, 0, 0, 1, 1, 0, 1, 0, 0, 0, 0, 0, 1, 0, 0, 0, 0, 1, 0, 0, 0, 0, 1, 0, 0, 0, 0, 0, 1, 1)$. Totally 645 birds from 72 species are recorded. Let us consider $\nu(d\lambda) = \gamma f(\lambda \mid \mu, \sigma) d\lambda$ where $f(\lambda \mid \mu, \sigma)$ is the density function of Lognormal(μ, σ^2) distribution. The parameter γ is the expected total number of species. From Section 3, the maximum likelihood estimate of μ and σ is identical to the conditional maximum likelihood estimate of the corresponding Poisson-lognormal model. The fitted lognormal mixing distribution is Lognormal($\hat{\mu}, \hat{\sigma}^2$) distribution with $\hat{\mu} = 1.23$ and $\hat{\sigma} = 1.30$. Let $\omega_i(\mu, \sigma) = P(Y = i)$ where Y is a Poisson-lognormal random variable with parameters μ and σ . We use the function “dpoilog” of R-package “poilog” to compute this probability. The estimated γ is $\hat{\gamma} = n_+(t_0)/(1 - \omega_0(\hat{\mu}, \hat{\sigma}^2)) = 85.2$.

Without loss of generality, set $t_0 = 1$. We use this data to investigate the information loss of the ρ -appearance design. The ρ -appearance data are simulated from the data using the following procedure:

Simulation procedure: Suppose species i has observed frequency m_i in time $[0, 1]$. If $m_i < \rho$, our data for this species is m_i , the frequency of it in time $[0, 1]$. If $m_i \geq \rho$, we simulate the ρ -appearance time of the species, r_i from Beta($\rho, m_i + 1 - \rho$) distribution, which is the distribution of the ρ order statistic of m_i samples from the $U(0, 1)$ distribution.

It can be shown that $E(N_k(t)) = \gamma \omega_k(\mu + \log(t), \sigma)$. The log-likelihood function is

$$\begin{aligned} & \log(\mathcal{L}(\gamma, \mu, \sigma \mid \{r_i, j_i\}_i)) \\ &= -\gamma(1 - \omega_0(\mu, \sigma)) + \sum_{k=1}^{\rho-1} n_k(1) \log(\gamma \omega_k(\mu, \sigma)) + \sum_{r_i < 1} \log(\gamma \omega_\rho(\mu + \log(r_i), \sigma)). \end{aligned}$$

Table A. Mean and standard deviation of estimators for North American breeding

	bird survey data (1995)						
ρ	1	2	3	4	5	6	∞
mean of $\hat{\mu}$	1.10	1.28	1.23	1.21	1.21	1.22	1.23
sd of $\hat{\mu}$	0.56	0.09	0.07	0.04	0.04	0.03	0*
mean of $\hat{\sigma}$	1.39	1.24	1.29	1.29	1.31	1.30	1.30
sd of $\hat{\sigma}$	0.48	0.15	0.13	0.08	0.09	0.07	0*
mean of $\hat{\gamma}$	90.4	83.8	85.0	85.5	85.7	85.3	85.2
sd of $\hat{\gamma}$	18.7	2.52	2.32	1.38	1.56	1.29	0*

* When $\rho = \infty$, we always observe the full data, and the sample standard deviation (sd) of the estimator across simulation is zero.

The maximum likelihood estimate for $E(N_+(1)) = \gamma(1 - \omega_0(\mu, \sigma))$ is $n_+(1)$. The function that we need to maximize to find $\hat{\mu}$ and $\hat{\sigma}$ is

$$h(\mu, \sigma) = -n_+(1) \log(1 - \omega_0(\mu, \sigma)) + \sum_{k=1}^{\rho-1} n_k(1) \log(\omega_k(\mu, \sigma)) + \sum_{r_i < 1} \log(\omega_\rho(\mu + \log(r_i), \sigma)).$$

The maximum likelihood estimate of γ is $\hat{\gamma} = n_+(1)/(1 - \omega_0(\hat{\mu}, \hat{\sigma}))$. We consider $\rho = 1, 2, \dots, 6$. For each ρ -value, we simulate 100 independent sets of ρ -appearance data. For each simulated data, μ , σ and γ are estimated. The sample mean and sample standard deviation of the estimates are presented in Table A. Graphical display is given in Fig. 3.

The mean of the estimate is close to that basing on $\tilde{n}(t_0)$. The standard deviation of the estimator decreases as ρ increases. We should avoid choosing $\rho = 1$, which is significantly inferior to $\rho = 2$. The effect of ρ on the standard deviation varies across parameters. Value $\rho = 4$ performs well for this data. The total number of species with frequency less than 4 is 33, around 46% of the seen species, and total number of individuals is 65, around 10% of the total number of individuals detected. If 4-appearance design is used, we need only to record about 10% of all seen individuals.

Appendix G: Comparison of MLE method and curve fitting method in extrapolation when finite number of points in the empirical SAC are available

We consider three distributions: power law, log-series distribution and geometric dis-

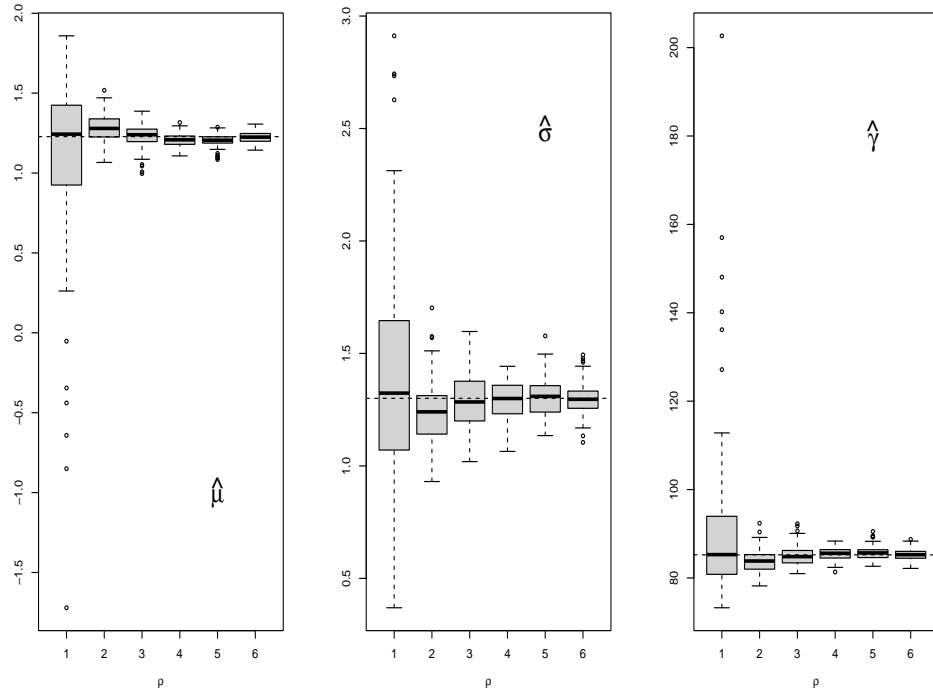


Figure 3: Box-and-whisker plots for estimators across different values of ρ in the simulation. The horizontal dashed line in each plot shows the estimate when the full Wisconsin route of the North American breeding bird survey data for 1995 is used. The variability of the estimate delineates the additional noise due to the ρ -appearance design.

tribution. The curve-fitting method of the distribution is described below:

- (a) Power law: $\psi(t) = \tau t^{1-1/c}$. For curve fitting, we regress $\log(\psi(t))$ on $\log(t)$.
- (b) Log-series distribution: $\psi(t) = \tau \log(1 + t/b) / \log(1 + 1/b)$. For curve fitting, we regress $\psi(t)$ on $\log(t)$. It is the standard approximation method which assumes that $1 + t/b \approx t/b$.
- (c) Geometric distribution (hyperbola law): $\psi(t) = \tau(1 + 2b)t/(t + 2b)$. There are various curve fitting methods for hyperbola law (see for example [Raaijmakers, 1987]). In this simulation, we use the simplest one, which regresses $1/\psi(t)$ on $1/t$.

With loss of generality, we set $t_0 = 1$. The parameter $\tau = \psi(1)$ is the expected number of recorded species at time $t_0 = 1$. In the experiment, τ can take value 200 and 1000. The distribution parameter can take 6 values. For power law, the value of c can be 1.25, 1.5, 2, 3, 4 and 5. For log-series distribution, the value of b can be 0.01, 0.02, 0.03, 0.05, 0.1, and 0.2. For geometric distribution, the value of b can be 0.05, 0.1, 0.2, 0.4, 0.6 and 0.8. Our data is $\{n_+(0.1), n_+(0.2), \dots, n_+(1)\}$. For each combination of parameters, we simulate 5000 data. The MLE estimate and curve-fitting estimate of $\psi(2)$ and $\psi(4)$ are found for each simulated data. We evaluate the performance of an estimator by the root mean squared relative error (RMSRE) (for estimator $\hat{\theta}$ for θ , $\text{RMSRE} = \left(\sqrt{\sum_{i=1}^n ((\hat{\theta}_i - \theta)/\theta)^2 / n} \right)$). The results of the simulation are presented in Tables B, C and D. The RMSRE for MLE is always smaller than that for the curve fitting method.

Table B. Simulation results for Power law

Extrapolate to $t = 2$, $\psi(1) = 200$						
c	1.25	1.5	2	3	4	5
RMSRE(Curve-fitting)	0.075	0.078	0.083	0.091	0.096	0.100
RMSRE(MLE)	0.073	0.074	0.077	0.080	0.082	0.083
Extrapolate to $t = 2$, $\psi(1) = 1000$						
c	1.25	1.5	2	3	4	5
RMSRE(Curve-fitting)	0.034	0.035	0.037	0.040	0.042	0.044
RMSRE(MLE)	0.033	0.034	0.035	0.036	0.037	0.037
Extrapolate to $t = 4$, $\psi(1) = 200$						
c	1.25	1.5	2	3	4	5
RMSRE(Curve-fitting)	0.081	0.089	0.103	0.120	0.132	0.140
RMSRE(MLE)	0.078	0.084	0.093	0.103	0.109	0.112
Extrapolate to $t = 4$, $\psi(1) = 1000$						
c	1.25	1.5	2	3	4	5
RMSRE(Curve-fitting)	0.036	0.040	0.045	0.052	0.057	0.060
RMSRE(MLE)	0.035	0.038	0.042	0.046	0.049	0.050

Table C. Simulation results for log-series distribution

Extrapolate to $t = 2$, $\psi(1) = 200$						
b	0.01	0.02	0.03	0.05	0.1	0.2
RMSRE(Curve-fitting)	0.073	0.073	0.073	0.077	0.090	0.122
RMSRE(MLE)	0.072	0.072	0.072	0.072	0.073	0.076
Extrapolate to $t = 2$, $\psi(1) = 1000$						
b	0.01	0.02	0.03	0.05	0.1	0.2
RMSRE(Curve-fitting)	0.033	0.034	0.036	0.043	0.065	0.106
RMSRE(MLE)	0.032	0.032	0.032	0.033	0.033	0.034
Extrapolate to $t = 4$, $\psi(1) = 200$						
b	0.01	0.02	0.03	0.05	0.1	0.2
RMSRE(Curve-fitting)	0.074	0.075	0.077	0.084	0.110	0.166
RMSRE(MLE)	0.073	0.074	0.074	0.076	0.079	0.086
Extrapolate to $t = 4$, $\psi(1) = 1000$						
b	0.01	0.02	0.03	0.05	0.1	0.2
RMSRE(Curve-fitting)	0.034	0.037	0.042	0.055	0.091	0.155
RMSRE(MLE)	0.033	0.033	0.034	0.034	0.035	0.038

Table D. Simulation results for geometric distribution

Extrapolate to $t = 2$, $\psi(1) = 200$						
b	0.05	0.1	0.2	0.4	0.6	0.8
RMSRE(Curve-fitting)	0.322	0.458	0.587	0.687	0.731	0.756
RMSRE(MLE)	0.085	0.106	0.136	0.165	0.174	0.174
Extrapolate to $t = 2$, $\psi(1) = 1000$						
b	0.05	0.1	0.2	0.4	0.6	0.8
RMSRE(Curve-fitting)	0.316	0.454	0.583	0.684	0.728	0.753
RMSRE(MLE)	0.054	0.079	0.111	0.134	0.136	0.132
Extrapolate to $t = 4$, $\psi(1) = 200$						
b	0.05	0.1	0.2	0.4	0.6	0.8
RMSRE(Curve-fitting)	0.320	0.462	0.601	0.716	0.768	0.798
RMSRE(MLE)	0.102	0.145	0.218	0.311	0.366	0.397
Extrapolate to $t = 4$, $\psi(1) = 1000$						
b	0.05	0.1	0.2	0.4	0.6	0.8
RMSRE(Curve-fitting)	0.315	0.458	0.598	0.713	0.766	0.796
RMSRE(MLE)	0.075	0.122	0.188	0.254	0.279	0.287

References

- Arrhenius, O. (1921). Species and area. *Journal of Ecology* **9**, 95–99.
- Béguinot, J. (2016). Extrapolation of the species accumulation curve associated to “chao” estimator of the number of unrecorded species: a mathematically consistent derivation. *Annual Research & Review in Biology* **11**, 1–19.
- Berger, J. O. and Berry, D. A. (1988). The relevance of stopping rules in statistical inference. In *Statistical Decision Theory and Related Topics: IV, Vol 1*, Eds. S. S. Gupta & J. O. Berger, pp.29–72. New York: Springer Verlag.
- Böhning, D. and Schön, D. (2005). Nonparametric maximum likelihood estimation of population size based on the counting distribution. *Journal of the Royal Statistical Society: Series C (Applied Statistics)* **54**, 721–737.

- Boneh, S., Boneh, A., and Caron, R. J. (1998). Estimating the prediction function and the number of unseen species in sampling with replacement. *Journal of the American Statistical Association* **93**, 372–379.
- Chao, A. (1984). Nonparametric estimation of the number of classes in a population. *Scandinavian Journal of Statistics* **11**, 265–270.
- Chee, C.-S. and Wang, Y. (2016). Nonparametric estimation of species richness using discrete k-monotone distributions. *Computational Statistics and Data Analysis* **93**, 107–118.
- Chiu, C.-H. and Chao, A. (2016). Estimating and comparing microbial diversity in the presence of sequencing errors. *PeerJ* **4**, 1634.
- Dengler, J. (2009). Which function describes the species–area relationship best? A review and empirical evaluation. *Journal of Biogeography* **36**, 728–744.
- Deolalikar, V. and Laffitte, H. (2016). Extensive large-scale study of error surfaces in sampling-based distinct value estimators for databases. *IEEE International Conference on Big Data* pp. 1579–1586.
- Dickie, I. A. (2010). Insidious effects of sequencing errors on perceived diversity in molecular surveys. *The New Phytologist* **188**, 916–918.
- Efron, B. and Thisted, R. (1976). Estimating the number of unseen species: How many words did Shakespeare know? *Biometrika* **63**, 435–447.
- Engen, S. (1974). On species frequency models. *Biometrika* **61**, 263–270.
- Favaro, S., Lijoi, A., Mena, R. H., and Prünster, I. (2009). Bayesian non-parametric inference for species variety with a two-parameter Poisson–Dirichlet process prior. *Journal of the Royal Statistical Society: Series B (Statistical Methodology)*, **71**, 993–1008.
- Fisher, R. A., Corbet, A. S., and Williams, C. B. (1943). The relation between the number of species and the number of individuals in a random sample of an animal population. *Journal of Animal Ecology* **12**, 42–58.

- Good, I. J. (1953). The population frequencies of species and the estimation of population parameters. *Biometrika* **40**, 237–264.
- Good, I. J. and Toulmin, G. (1956). The number of new species, and the increase in population coverage, when a sample is increased. *Biometrika* **43**, 45–63.
- Haas, P. J., Naughton, J. F., Seshadri, S., and Stokes, L. (1995). Sampling-based estimation of the number of distinct values of a attribute. *VLDB* **95**, 311–322.
- Kingman, J. F. C. (1993). *Poisson Processes*. Oxford: Oxford University Press.
- Kobayashi, S. (1975). The species-area relation ii. a second model for continuous sampling. *Researches on Population Ecology* **16**, 265–280.
- Lijoi, A., Mena, R. H. and Prünster, I. (2007). Bayesian nonparametric estimation of the probability of discovering new species. *Biometrika* **94**, 769–786.
- Magurran, A. E. (2007). Species abundance distributions over time. *Ecology Letters* **10**, 347–354.
- Martin, H. G. and Goldenfield, N. (2006). On the origin and robustness of power-law species-area relationships in ecology. *PNAS* **103**, 10310–10315.
- Matthews, T. J. and Whittaker, R. J. (2014). Fitting and comparing competing models of the species abundance distribution: assessment and prospect. *Frontiers of Biogeography* **6**, 67–82.
- Matthews, T. J. and Whittaker, R. J. (2015). On the species abundance distribution in applied ecology and biodiversity management. *Journal of Applied Ecology* **52**, 443–454.
- May, R. M. (1975). Patterns of species abundance and diversity. In *Ecology and Evolution of Communities*, Eds. M. L. Cody & J. M. Diamond, pp.81–120. Cambridge: Belknap Press.
- McGill, B. J., Etienne, R. S., Gray, J. S., Alonso, D., Anderson, M. J., Benecha, H. K., Dornelas, M., Enquist, B. J., Green, J. L., He, F., Hurlbert, A. H., Magurran, A. E., Marquet, P. A., Maurer, B. A., Ostling, A., Soykan, C. U., Ugland, K. I.,

- and White, E. P. (2007). Species abundance distributions: moving beyond single prediction theories to integration within an ecological framework. *Ecology Letters* **10**, 995–1015.
- Norris, J. L. and Pollock, K. H. (1998). Non-parametric MLE for Poisson species abundance models allowing for heterogeneity between species. *Environmental and Ecological Statistics* **5**, 391–402.
- Novotny, V. and Basset, Y. (2000). Rare species in communities of tropical insect herbivores: pondering the mystery of singletons. *Oikos* **89**, 564–572.
- Preston, F. W. (1960). Time and space and the variation of species. *Ecology* **41**, 612–627.
- Preston, F. W. (1962). The canonical distribution of commonness and rarity. *Ecology* **43**, 185–215.
- Quince, C., Lanzen, A., Davenport, R. J., and Turnbaugh, P. J. (2011). Removing noise from pyrosequenced amplicons. *BMC Bioinformatics* **12**, 38.
- Raaijmakers, J. G. W. (1987). Statistical analysis of the Michaelis-Menten equation. *Biometrics* 793–803.
- Raiffa, H., and Schlaifer, R. (1961). *Applied Statistical Decision Theory*. Boston: Division of Research, Graduate School of Business Administration, Harvard Univer.
- Scheiner, S. M. (2003). Six types of species-area curves. *Global Ecology & Biogeography* **12**, 441–447.
- Schilling, R. L., Song, R., and Vondracek, Z. (2012). *Bernstein Functions: Theory and Applications*. Walter de Gruyter.
- Tjørve, E. (2003). Shapes and functions of species-area curves: a review of possible models. *Journal of Biogeography* **30**, 827–835.
- Tjørve, E. (2009). Shapes and functions of species-area curves (ii): a review of new models and parameterizations. *Journal of Biogeography* **36**, 1435–1445.

- Trushkowsky, B., Kraska, T., Franklin, M. J., and Sarkar, P. (2012). Getting it all from the crowd. arXiv preprint arXiv:1202.2335.
- Wang, J.-P. (2010). Estimating species richness by a Poisson-compound gamma model. *Biometrika* **97**, 727–740.
- Williams, M. R., Lamont, B. B., and Henstridge, J. D. (2009). Species-area functions revisited. *Journal of Biogeography* **36**, 1994–2004.
- Zhou, M., Favaro, S., and Walker, S. G. (2017). Frequency of frequencies distributions and size-dependent exchangeable random partitions. *Journal of the American Statistical Association* **112**, 1623–1635.